

Majorana Spin Current Generation by Dynamic Strain

Yuki Yamazaki,¹ Takumi Funato,^{2,3} and Ai Yamakage¹

¹*Department of Physics, Nagoya University, Nagoya 464-8602, Japan*

²*Center for Spintronics Research Network, Keio University, Yokohama 223-8522, Japan*

³*Kavli Institute for Theoretical Sciences, University of Chinese Academy of Sciences, Beijing, 100190, China*

(Dated: January 12, 2023)

Majorana fermions that emerge on the surface of topological superconductors are charge neutral but can have higher-rank electric multipoles by allowing for account time-reversal and crystalline symmetries. Applying the general classification of these multipoles, we show that the spin current of Majorana fermions is driven by spatially nonuniform dynamic strains on the (001) surface of superconducting antiperovskite Sr_3SnO . We also find that the frequency dependence of the Majorana spin current reflects the energy dispersion of Majorana fermions. Our results suggest that the spin current can be a probe for Majorana fermions.

Majorana fermions (MFs) are charge-neutral relativistic particles moving in 3D space. In addition, two types of MFs emerge in topological superconductors (TSCs) as gapless Andreev bound states [1–7]. One type is a spatially localized zero-dimensional MF, which appears at the ends of nanowires [8–14] or in the cores of the vortices of TSCs [15–18]. MFs have been the subject of considerable research because of their potential application to fault-tolerant topological quantum computation with non-Abelian statistics [19, 20].

Here, one can ask the following question: what are the physical phenomena unique to spatially extended 1D or 2D MFs? A typical example is a half-integer thermal quantum Hall effect on the surface of a TSC [21–23]. “Half-Integer” is a peculiarity originating from the fact that MFs are heat carriers. The half-integer thermal quantum Hall effect is unique to MFs that are spread in 2D space and uses the thermal gradient as the “driving force”. Recently, the optical response of Majorana chiral edge modes has also been discussed [24, 25]. The frequency dependence of real-part optical conductivity is proportional to ω^2 , where it can be distinguished from trivial superconductors or insulators and Dirac chiral edge modes. Then, the driving force of MFs is an electromagnetic wave. In superconductors, we cannot use an electric field to survey superconducting properties since charge conservation is broken. The responses to acoustic waves have been studied extensively through measurements of ultrasonic attenuation [26, 27] to investigate superconducting symmetry or measurements of the temperature dependence of a superconducting gap [28]. Therefore, we can expect to be able to use dynamic strains for the driving force of MFs on the surfaces of 3D TSCs.

When MFs have time-reversal symmetry, they do not appear alone but form Kramers pairs, which are called MKPs. Due to the time-reversal symmetry, a single MKP is stable against an electrical external field such as acoustic waves with lattice strains. Previously, we derived the general effective theory for electromagnetic properties of “double” MKPs on a surface of a 3D TSC [29–31]. Double MKPs can have various electrical multipole degrees of freedom that are qualitatively different from those of ordinary fermions, and it has been shown that they can respond to static strains [31]. Double MKPs are always protected by crystalline symmetries in addi-

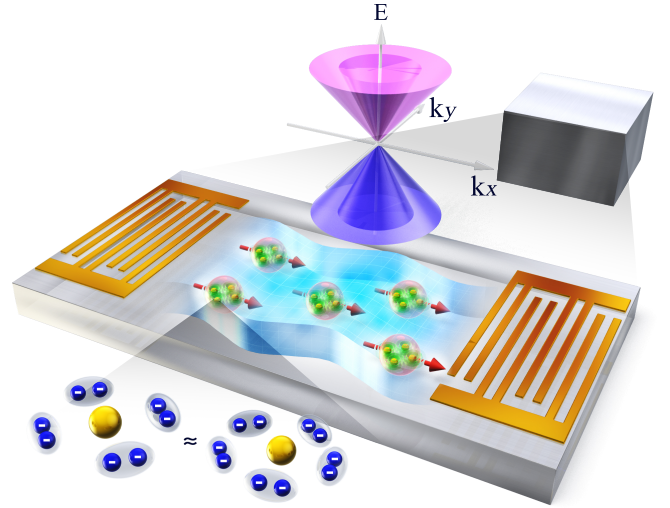


FIG. 1. This schematic shows that the Majorana spin currents flow on the surface of the 3D TCSC driven by a dynamic strain. The surface has four Majorana fermions that form double Majorana Kramers pairs (MKPs). Double MKPs have electric quadrupoles coupled to a dynamic strain, and the spin current of Majorana electric quadrupoles is generated by a dynamic strain.

tion to time-reversal symmetry; thus, TSCs are specifically referred to as topological crystalline superconductors (TCSCs).

In this letter, we clarify the transport phenomena of double MKPs driven by spatially nonuniform dynamic strains on the surface of 3D TCSCs. We consider the surface of the antiperovskite TCSC Sr_3SnO [32], which has double MKPs with two electrical multipoles on its (001) surface [31, 33]. We start with a 4×4 Dirac Hamiltonian with respect to the (001) surface point group (PG) symmetry. Then, we reveal the spin current of double MKPs, referred to as the “Majorana spin current”, generated by spatially nonuniform dynamic strains on the surface (see Fig. 1). When there is no gap in the dispersion of double MKPs, we find that the Majorana spin current is caused by an intrinsic effect and does not depend on relaxation times. Alternatively, for the gapped case induced by surface magnetization, the Majorana spin current has two frequency regions that reflect the energy dispersion of double MKPs. Our study suggests that the measurement of the Majorana spin current can be a new probe for Majorana fermion

TABLE I. Irreducible decomposition of the matrices, momentum, strain, and spin current in the $p4m$ model for the A_{1u} superconducting pair potential in the bulk. The matrix is transformed by g as $\eta \rightarrow D_g^\dagger \eta D_g$. (η_i, η_j) denotes $(\eta_i, \eta_j) \rightarrow (-\eta_j, \eta_i)$ by transformation of C_{4z} and $(\eta_i, \eta_j) \rightarrow (-\eta_i, \eta_j)$ by transformation of $\sigma(xz)$. Electric/magnetic and PHS denote time-reversal even/odd and particle-hole symmetry, respectively. $u_{ij}(\mathbf{x}) = \partial_i u_j(\mathbf{x})$ with \mathbf{u} the displacement field. j_i^α denotes spin $\sigma^\alpha/2$ current along the i th direction.

IR	electric w/ PHS	electric w/o PHS	magnetic w/ PHS	magnetic w/o PHS	momentum	strain	spin current
A_1		$s_0\tau_0, s_0\tau_3$			$k_x^2 + k_y^2$	$u_{xx} + u_{yy}$	$J_y^x - J_x^y$
A_2			$s_3\tau_0, s_3\tau_3$			$u_{xy} - u_{yx}$	$J_x^x + J_y^y$
B_1	$s_3\tau_1$			$s_3\tau_2$	$k_x^2 - k_y^2$	$u_{xx} - u_{yy}$	$J_y^x + J_x^y$
B_2	$s_0\tau_2$			$s_0\tau_1$	$k_x k_y$	$u_{xy} + u_{yx}$	$J_x^x - J_y^y$
E		$(s_1\tau_1, s_2\tau_1)$	(η_5, η_6)	$(\eta_1, \eta_2), (\eta_3, \eta_4)$	(k_x, k_y)	(u_{xz}, u_{yz})	$(J_y^z, -J_x^z)$

observation.

Before we consider the main topic, we discuss the electromagnetic properties of MKPs on the surface of a TSC. When there is only one MF on the surface, the single MF is strongly protected by particle-hole symmetry (charge-neutrality constraint), and it is extremely stable against any external fields. If a TSC has time-reversal symmetry, then the two MFs form an MKP. The single MKP is protected by time-reversal symmetry, and hence, it generally responds only to magnetic external fields and remains stable to electrical external fields. On the other hand, when crystalline symmetries are taken into account, there can exist double MKPs, and they can respond to an electrical perturbation that breaks the crystalline symmetry. The coupling of N MKPs to a spatially uniform external field can be represented by Ref. [31]

$$\hat{H}_{\text{surf,ex}} = -\hat{O}F, \quad \hat{O} = \frac{1}{2} \int d^2x \sum_{ss'} \hat{\psi}_s(\mathbf{x}) (A_F)_{ss'} \hat{\psi}_{s'}(\mathbf{x}), \quad (1)$$

where $\hat{\psi}_s(\mathbf{x})$ ($s = 1, \dots, 2N$) are Majorana field operators and satisfy $\hat{\psi}_s^\dagger(\mathbf{x}) = \hat{\psi}_s(\mathbf{x})$. A_F is conjugate to F and should be an antisymmetric Hermite matrix since Majorana field operators obey $\{\hat{\psi}_s(\mathbf{x}), \hat{\psi}_{s'}(\mathbf{x}')\} = \delta_{ss'} \delta^2(\mathbf{x} - \mathbf{x}')$. When A_F is the 2×2 matrix, with only one MKP, there exists only $A_F = \sigma_y$, which satisfies $\Theta_{\text{surf}} A_F \Theta_{\text{surf}}^{-1} = -A_F$ for the time-reversal operator $\Theta_{\text{surf}} = (-i\sigma_y K)$. K is a complex conjugation, and hence, the MKP couples only to magnetic external fields. On the other hand, when A_F is the 4×4 matrix, with double MKPs, A_F , which satisfies $\Theta_{\text{surf}} A_F \Theta_{\text{surf}}^{-1} = A_F$, can be formed, and the double MKPs can also be coupled to the electrical external field by Eq. (1). Double MKPs have various electric multipoles depending on each crystalline symmetry of the surface, i.e., wall-paper groups (WGs), and superconducting symmetries. In a previous study [31], we revealed the coupling between the electric multipoles and the spatially uniform static strain for each WGs.

We consider the antiperovskite superconductor Sr_3SnO as a concrete model. Antiperovskite A_3BX , $A = \text{Ca, Sr, La}$, $B = \text{Pb, Sn}$, $X = \text{C, N, O}$ with the space group symmetry $Pm\bar{3}m$ (No.221) [34, 35], has multiple $J = 3/2$ bands and is a candidate material for topological crystalline insulators due to the band inversion of two orbitals [36–38]. In particular, Sr_3SnO has the potential to become a TSC with hole doping

at temperatures below 5 K [32]. Interestingly, it has been suggested that double MKPs can appear in the (001) surface with $p4m$ WG symmetry when the superconductor symmetry is in the A_{1u} representation in bulk with O_h PG symmetry [33]. In the following, we consider the double MKPs on the (001) surface in the A_{1u} state of Sr_3SnO and derive the Majorana spin current generated by spatially nonuniform dynamic strains.

To analyze the transport properties of double MKPs, we utilize the low-energy Dirac model for the (001) surface of Sr_3SnO with $p4m$ WG symmetry, which equals C_{4v} PG symmetry. The surface symmetry operations are given by $D_{\{C_{4z}|0\}} = \frac{-1}{\sqrt{2}}(s_0\tau_3 - is_3\tau_3)$ and $D_{\{\sigma(xz)|0\}} = \frac{i}{\sqrt{2}}(s_2\tau_3 - s_1\tau_3)$ with D_g being a representation matrix of $g \in C_{4v}$, where $s_i\tau_j$'s are the product of Pauli matrices acting on the spin, orbital, and sublattice degrees of freedom. Then, we obtain the total symmetric Hamiltonian [30, 31]. (see Table I and Sec. I of Supplemental Material [39]):

$$\hat{H} = \frac{1}{2} \sum_{\mathbf{k}} \hat{\psi}_{\mathbf{k}}^\dagger H(\mathbf{k}) \hat{\psi}_{\mathbf{k}},$$

$$H(\mathbf{k}) = [v_1(\eta_1 k_y - \eta_2 k_x) + v_2(\eta_3 k_y - \eta_4 k_x)], \quad (2)$$

where $\hat{\psi}_{\mathbf{k}}^\dagger = (\hat{\psi}_{1\mathbf{k}}^\dagger, \hat{\psi}_{2\mathbf{k}}^\dagger, \hat{\psi}_{3\mathbf{k}}^\dagger, \hat{\psi}_{4\mathbf{k}}^\dagger)$ and $\hat{\psi}_{\mathbf{k}} = {}^t(\hat{\psi}_{1\mathbf{k}}, \dots, \hat{\psi}_{4\mathbf{k}})$ are the Majorana creation/annihilation operators, which satisfy $\hat{\psi}_{1\mathbf{k}}^\dagger = \hat{\psi}_{2-\mathbf{k}}, \hat{\psi}_{3\mathbf{k}}^\dagger = \hat{\psi}_{4-\mathbf{k}}$ and the subscripts 1, ..., 4 denote four MFs. η_i 's are given by $\eta_1 = (1/\sqrt{2})(s_1\tau_0 + s_2\tau_0), \eta_2 = (-1/\sqrt{2})(s_1\tau_0 - s_2\tau_0), \eta_3 = (1/\sqrt{2})(s_1\tau_3 + s_2\tau_3), \eta_4 = (-1/\sqrt{2})(s_1\tau_3 - s_2\tau_3)$. $H(\mathbf{k})$ satisfies $D_g H(\mathbf{k}) D_g^\dagger = H(g\mathbf{k})$ where a momentum \mathbf{k} is transformed to $g\mathbf{k}$ under the action of g . The spin of MFs is represented by $\boldsymbol{\sigma} = (\sigma_x, \sigma_y, \sigma_z) \equiv (\eta_5, \eta_6, -s_3\tau_0)$ where $\eta_5 = (1/\sqrt{2})(s_1\tau_2 - s_2\tau_2), \eta_6 = (-1/\sqrt{2})(s_1\tau_2 + s_2\tau_2)$, which are coupled to the magnetization \mathbf{M} as $\mathbf{M} \cdot \boldsymbol{\sigma}$. The time-reversal Θ , particle-hole C , and chiral Γ symmetries are defined by $\Theta = s_2\tau_3 K, C = s_1\tau_0 K, \Gamma = s_3\tau_3$ where they satisfy $\Theta H(\mathbf{k}) \Theta^{-1} = H(-\mathbf{k}), CH(\mathbf{k})C^{-1} = -H(-\mathbf{k}), \Gamma H(\mathbf{k}) \Gamma^{-1} = -H(\mathbf{k})$. In our model, which is the C_{4v} PG symmetric model for the A_{1u} bulk's superconducting pair potential with O_h PG symmetry, the double MKPs have specific electromagnetic multipoles with particle-hole symmetry. Table I shows that the double MKPs have magnetic multipoles that are represented by $\boldsymbol{\sigma}$ and electric multipoles that are represented by $s_3\tau_1$ with B_1 and $s_0\tau_2$ with B_2 representations. Therefore, as follows, we can

define the spin currents $j_y^x + j_x^y$ and $j_x^x - j_y^y$ generated by dynamical strains $u_{xx} - u_{yy}$ and $u_{xy} + u_{yx}$, where $u_{ij}(\mathbf{x}) = \partial_i u_j(\mathbf{x})$ and $u_j(\mathbf{x}) \propto e^{i(\mathbf{q}\cdot\mathbf{x} - \omega t)}$ denote the displacement field, respectively (Fig. 1). For double MKPs, we can construct the spin current operator only from surface effective theory, i.e., the spin current is defined by $j_i^\alpha \equiv \frac{1}{2}\{\sigma_\alpha, \partial H(\mathbf{k})/\partial k_i\}$ ($i = x, y$), which satisfies particle-hole symmetry $C j_i^\alpha C^{-1} = -j_i^\alpha$. Then, we obtain $\hat{j}_y^x(\mathbf{q}) + \hat{j}_x^y(\mathbf{q}) = \frac{1}{2} \sum_k \hat{\psi}_{k-\frac{q}{2}}^\dagger [-v_2 s_3 \tau_1] \hat{\psi}_{k+\frac{q}{2}}$ and $\hat{j}_x^x(\mathbf{q}) - \hat{j}_y^y(\mathbf{q}) = \frac{1}{2} \sum_k \hat{\psi}_{k-\frac{q}{2}}^\dagger [v_1 s_0 \tau_2] \hat{\psi}_{k+\frac{q}{2}}$.

Here, we define the operators, which are represented by $\hat{O}^{(1)}(\mathbf{q}) \equiv \frac{1}{2} \sum_k \hat{\psi}_{k-\frac{q}{2}}^\dagger (\rho_1 s_3 \tau_1) \hat{\psi}_{k+\frac{q}{2}}$ and $\hat{O}^{(2)}(\mathbf{q}) \equiv \frac{1}{2} \sum_k \hat{\psi}_{k-\frac{q}{2}}^\dagger (\rho_2 s_0 \tau_2) \hat{\psi}_{k+\frac{q}{2}}$. Since $\hat{O}^{(1)}$ and $u_{xx} - u_{yy}$, $\hat{O}^{(2)}$ and $u_{xy} + u_{yx}$ share the same representation, the couplings between double MKPs and the dynamical strains are represented by

$$\hat{H}_{\text{surf,ex}} = - \left\{ \hat{O}^{(1)}(\mathbf{q}) [u_{xx}(\mathbf{q}, \omega) - u_{yy}(\mathbf{q}, \omega)] + \hat{O}^{(2)}(\mathbf{q}) [u_{xy}(\mathbf{q}, \omega) + u_{yx}(\mathbf{q}, \omega)] \right\}. \quad (3)$$

Then, we calculate the linear response of the spin currents $\hat{j}_y^x + \hat{j}_x^y$ and $\hat{j}_x^x - \hat{j}_y^y$ to the dynamic strains given by Eq. (3):

$$\langle \hat{j}_y^x + \hat{j}_x^y \rangle(\mathbf{q}, \omega) \equiv K_1(\mathbf{q}, \omega) [u_{xx}(\mathbf{q}, \omega) - u_{yy}(\mathbf{q}, \omega)] + K_2(\mathbf{q}, \omega) [u_{xy}(\mathbf{q}, \omega) + u_{yx}(\mathbf{q}, \omega)], \quad (4)$$

$$\langle \hat{j}_x^x - \hat{j}_y^y \rangle(\mathbf{q}, \omega) \equiv K'_1(\mathbf{q}, \omega) [u_{xx}(\mathbf{q}, \omega) - u_{yy}(\mathbf{q}, \omega)] + K'_2(\mathbf{q}, \omega) [u_{xy}(\mathbf{q}, \omega) + u_{yx}(\mathbf{q}, \omega)], \quad (5)$$

where the response function $K_i(\mathbf{q}, \omega)$ is given by Ref. [40]

$$K_i(\mathbf{q}, \omega) \equiv i \int_0^\infty dt e^{i(\omega+i\delta)t} \langle [\hat{j}_y^x(\mathbf{q}, t) + \hat{j}_x^y(\mathbf{q}, t), \hat{O}^{(i)}(-\mathbf{q}, 0)] \rangle, \quad (6)$$

where $\hat{A}(t) = e^{i\hat{H}t} \hat{A} e^{-i\hat{H}t}$ and $\delta \rightarrow +0$. $K'_i(\mathbf{q}, \omega)$ is also defined by replacing $\hat{j}_y^x + \hat{j}_x^y$ with $\hat{j}_x^x - \hat{j}_y^y$ in Eq. (6). Note that the chemical potential μ for MFs is equal to 0 due to particle-hole symmetry in superconducting states. Additionally, $\langle \dots \rangle = \text{tr}[e^{-\hat{H}/T} \dots] / \text{tr}[e^{-\hat{H}/T}]$. If there are no applied external fields, $K_1(\mathbf{q}, \omega)$ and $K'_2(\mathbf{q}, \omega)$ then only take finite values since the spin currents and dynamic strains share the same representation of C_{4v} . Here, we assume that the wavenumber q and the frequency ω are smaller than the mean free path l and relaxation time τ of the MFs. These conditions are represented by $q \ll l^{-1}$, $\omega \ll \tau^{-1} = 2\gamma$. We expand the response function for ω and consider the nonequilibrium part: $K_i(\omega) - K_i(0)$. (the details are shown in Sec. II of the Supplemental Material [39]):

$$K_1(\omega) - K_1(0) \simeq \frac{i\omega}{8\pi^2} \frac{\rho_1}{v_1} \ln \left[\frac{(v_1 - v_2)^2}{(v_1 + v_2)^2} \right]. \quad (7)$$

One can see that $K_1(\omega) - K_1(0)$ is independent of the damping parameter γ . Note that $K'_2(\omega) - K'_2(0) = \frac{v_1 \rho_2}{-v_2 \rho_1} (K_1(\omega) - K_1(0))$

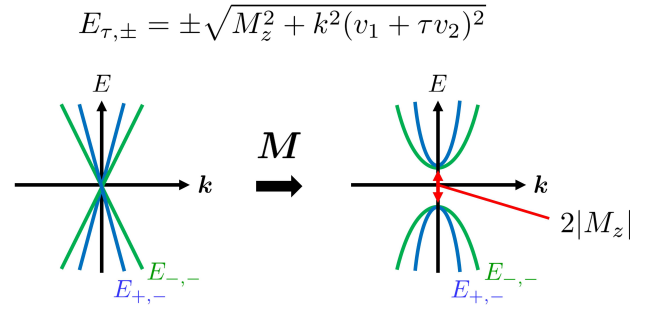


FIG. 2. The energy dispersion of (left) Eq. (2) and (right) Eq. (8). The energy gap opened by the magnetization M .

because of chiral symmetry. The details are shown in Sec. II of the Supplemental Material [39].

Next, we consider the case in which the dispersion of double MKPs is gapped. This situation can be realized, for example, by attaching ferromagnets on the surface. Then, the effective Hamiltonian is given by

$$\tilde{H}(\mathbf{k}) = H(\mathbf{k}) + \tilde{M}_z \sigma_z. \quad (8)$$

The second term in Eq. (8) is the Zeeman term reflected by coupling between the spin moment of double MKPs and the magnetization of ferromagnets, where we define $M_z \equiv -\tilde{M}_z$. Then, the energy dispersion is given by $E_{\tau=\pm, \pm} = \pm \sqrt{M_z^2 + k^2(v_1 + \tau v_2)^2}$ in Fig. 2. The applied magnetization opens an energy gap in the dispersion of double MKPs and lowers the symmetry from C_{4v} to C_4 . Therefore, $K_2(\omega)$ can take a finite value since $j_y^x + j_x^y$ and $u_{xy} + u_{yx}$ share the same irreducible representation of C_4 . The relationship between B_z and ω , is important; hence, we calculate the response function by using the Lehmann representation when the dispersion of double MKPs is gapped:

$$K_1(\omega) = \frac{1}{4} \sum_{n \in \text{occ}, m \in \text{unocc}} \left\{ \frac{\langle n | -v_2 s_3 \tau_1 | m \rangle \langle m | \rho_1 s_3 \tau_1 | n \rangle}{E_n - E_m + \omega + i\delta} + \left[\frac{\langle n | -v_2 s_3 \tau_1 | m \rangle \langle m | \rho_1 s_3 \tau_1 | n \rangle}{E_n - E_m - \omega + i\delta} \right]^* \right\}, \quad (9)$$

$$K_2(\omega) = \frac{1}{4} \sum_{n \in \text{occ}, m \in \text{unocc}} \left\{ \frac{\langle n | -v_2 s_3 \tau_1 | m \rangle \langle m | \rho_2 s_0 \tau_2 | n \rangle}{E_n - E_m + \omega + i\delta} + \left[\frac{\langle n | -v_2 s_3 \tau_1 | m \rangle \langle m | \rho_2 s_0 \tau_2 | n \rangle}{E_n - E_m - \omega + i\delta} \right]^* \right\}. \quad (10)$$

where $\delta \rightarrow +0$, $|n\rangle$ and $|m\rangle$ denote occupied states and unoccupied states of Eq. (8), respectively. As a result, we obtain

TABLE II. Electromagnetic degrees of freedom of the double Majorana Kramers pairs (MKPs). They emerge on the surface with wallpaper-group (WG) symmetry, when the bulk pair potential belongs to irrep Δ . Irreps of double MKPs, magnetic operators, electric operators of MKPs, which couple to magnetization M_z perpendicular to the surface and strain $[u_{ij}(\mathbf{x}) = \partial_i u_j(\mathbf{x})]$, where $\mathbf{u}(\mathbf{x})$ denotes the displacement field, are also shown. The last column denotes that the strain can couple to the double MKPs and the generated spin current by the strain. We adapt the definition for WG and irreps by Bilbao Crystallographic Server [41]. $\bar{\Gamma}_i$ denotes the i th double-valued irrep of the little group on the Γ point. $2\bar{\Gamma}_i = \bar{\Gamma}_i \oplus \bar{\Gamma}_i$. The result for $P3m1$ are the same as that for $P31m$.

WG	Δ	MKPs	Magnetic	Electric	Magnetization M_z	Strain (Spin current)	
						$u_{xx} - u_{yy} (j_y^x + j_x^y)$	$u_{xy} + u_{yx} (j_x^x - j_y^y)$
$p4m$	A_2	$\bar{\Gamma}_6 \oplus \bar{\Gamma}_7$	$2A_2 + E$	$B_1 + B_2$	gapped	\circ	\circ
$p31m$	A_1	$2(\bar{\Gamma}_4 \oplus \bar{\Gamma}_5)$	$4A_1$	$2A_2$	gapless	\times , only coupled to $u_{xy} - u_{yx} (j_x^x + j_y^y)$	\circ
$p4g$	B_1	$\bar{M}_6 \oplus \bar{M}_7$	$A_2 + B_1 + E$	$A_2 + B_2$	gapped	\times , coupled to $u_{xy} - u_{yx} (j_x^x + j_y^y)$	\circ

the nonequilibrium part: $K_i(\omega) - K_i(0)$.

$$K_1(\omega) - K_1(0) = \begin{cases} \frac{A\omega^2}{M_z} & (\omega \ll 2|M_z|), \\ B \left(-\frac{\omega}{2} \ln \left| \frac{1 + \frac{2k_c v_1}{\omega}}{1 - \frac{2k_c v_1}{\omega}} \right| + \frac{2M_z v_1^2}{v_1^2 - v_2^2} - \frac{M_z v_1 \ln \left| \frac{v_1 - v_2}{v_1 + v_2} \right|}{2v_2} \right) + i \frac{B\pi v_1}{2v_2} \omega & (2|M_z| \ll \omega \ll x(k_c)), \end{cases} \quad (11)$$

$$K_2(\omega) - K_2(0) = \begin{cases} iC\omega & (\omega \ll 2|M_z|), \\ D\pi M_z + iDM_z \ln \left| \frac{1 + \frac{2k_c v_1}{\omega}}{1 - \frac{2k_c v_1}{\omega}} \right| & (2|M_z| \ll \omega \ll x(k_c)), \end{cases} \quad (12)$$

$$A = \frac{2v_1 v_2 (3v_2^2 - v_1^2) - ((v_1^2 + v_2^2)^2 - 4v_2^4) \ln \left| \frac{v_1 - v_2}{v_1 + v_2} \right|}{32v_1^3 v_2^3}, \quad B = \frac{v_2 \rho_1}{8\pi v_1^2},$$

$$C = \frac{v_2 \rho_2}{4\pi} \frac{-2v_1 v_2 + v_2^2 \ln \left| \frac{v_1 + v_2}{v_1 - v_2} \right|}{8v_1^2 v_2^2}, \quad D = -\frac{v_2 \rho_2}{8\pi} \frac{v_2}{v_1^3 - v_1 v_2^2}, \quad (13)$$

where $x(k_c) = \sqrt{M_z^2 + k_c^2(v_1 + v_2)^2} + \sqrt{M_z^2 + k_c^2(v_1 - v_2)^2}$ and k_c is a cutoff value (see Sec. II of the Supplemental Material for detailed results [39]). Eqs. (11) and (12) show that $K_1(\omega)$ and $K_2(\omega)$ have two frequency regions with different behaviors. The numerical results of Eqs. (9) and (10) are shown in Fig. 3, and they reproduce the approximate analytical solutions obtained in each region well. Both $K_1(\omega) - K_1(0)$ and $K_2(\omega) - K_2(0)$ reflect the energy dispersion of the MFs. In particular, there are abrupt changes in the values of (a), (b), and (c) in Fig. 3, which are the points at $\omega = 2|M_z|$, just when the frequency is equal to the band gap. On the other hand, (d) is the diagram corresponding to the result of the principal value integration in Eq. (10), and there is no peak structure even at $\omega = 2|M_z|$ where the density of states becomes finite. This is because the chemical potential of MFs is exactly zero, and $K_2(\omega) - K_2(0)$ is the quantity that can take a finite value when the dispersion of MFs exhibits an energy gap with applied magnetization. Hence, the contribution from the Fermi sea is considered to be dominant.

In this letter, we show that the Majorana spin current generated by spatially nonuniform dynamic strain flows on the (001) surface of the 3D time-reversal-invariance TCSC Sr_3SnO . For the gapless case, the spin current does not show

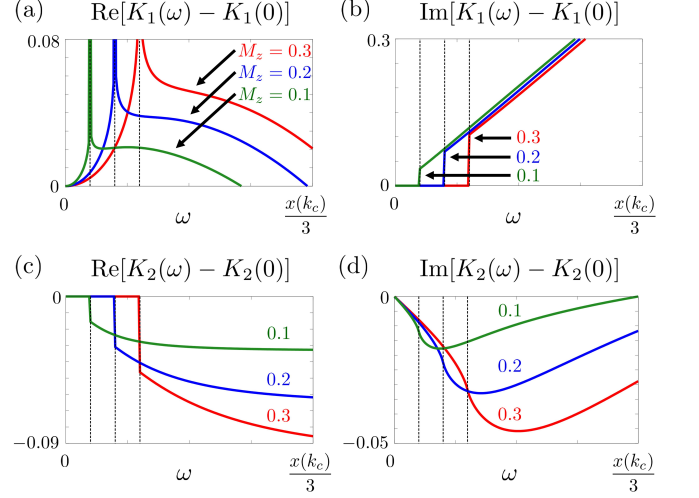


FIG. 3. The numerical results of Eqs. (9) and (10). (a) and (b) show the amplitudes of the real and imaginary parts of $K_1(\omega) - K_1(0)$, respectively. (c) and (d) show the real and imaginary parts of $K_2(\omega) - K_2(0)$, respectively. Red, blue and green lines denote the cases of $|M_z| = 0.3$, $|M_z| = 0.2$ and $|M_z| = 0.1$, respectively. The values of the three black dotted lines drawn on the horizontal axis in (a), (b), (c), and (d) denote the size of the energy gap $2|M_z|$, and from left to right are 0.2, 0.4, and 0.6. The parameters are $\rho_1 = 1.0, \rho_2 = 1.0, v_1 = 0.3, v_2 = 0.2, k_c = 10$.

damping dependence due to the linear dispersion of the double MKPs and the fact that their chemical potential is exactly zero. In contrast, for the gapped case, the spin currents reflect the energy dispersion of the MFs, and they have a unique frequency dependence. We emphasize again that the electromagnetic multipoles formed by double MKPs determine the properties of the spin current responses to dynamic strains. To see this, we show the results of the previous study [31] in Table II (See the Supplemental material of Ref. [31] for the complete version). This table shows the electromagnetic degrees of freedom of double MKPs for several WGs, irreps of the pair potential, and double MKPs. The case of $p4m$ corresponds to the present model. In the case of $p4m$ and $p4g$, the applied magnetization M_z induces the energy gap of double MKPs; however, in the case of $p31m$, the double MKPs still remain gapless. In addition, $p4m$ and $p4g$ are the same gapped case, but in the case of $p4g$, the double MKPs do not couple to

the strain $u_{xx} - u_{yy}$ but couple to $u_{xy} - u_{yx}$ owing to the protection of glide-plane symmetry. We have specifically shown the application of the general effective theory for the electromagnetic properties of surface double MKPs derived from system symmetries, such as crystalline and superconducting symmetries, and the new dynamics of MFs characterized by these symmetries. We believe that our work accelerates the study of the coupling of given external fields with MFs and the transport phenomena arising therefrom.

As a detection method for AC spin currents, spin wave resonance can be observed by injecting spin currents into ferromagnetic metals [42, 43] and the rectifying effect of magnetostriction [44]. The dynamic strains $u_{xx}(\mathbf{r}, t)$ and $u_{xy}(\mathbf{r}, t)$ can be realized by a Rayleigh wave and a Love wave propagating in the x -direction, respectively. In relation to the experiment, parameters such as ρ_1, ρ_2, v_1, v_2 can be obtained by projecting bulk operators onto the surface. This study will be published in a future paper.

The authors gratefully acknowledge M. Matsuo, Y. Nozaki, J. J. Nakane, Y. Imai, T. Yamaguchi, T. Matsushita, R. Kikuchi, and H. Kohno for valuable discussions. This work was supported by JSPS KAKENHI for Grants (No. JP20K03835) and the Sumitomo Foundation (190228). Y.Y. is supported by Grant-in-Aid for JSPS Fellows Grant No. 22J14452. This work was financially supported by JST SPRING, Grant Number JPMJSP2125. The author Y.Y. would like to take this opportunity to thank the ‘‘Interdisciplinary Frontier Next-Generation Researcher Program of the Tokai Higher Education and Research System.’’

-
- [1] C.-R. Hu, Midgap surface states as a novel signature for $d_{x^2-y^2}$ -wave superconductivity, *Phys. Rev. Lett.* **72**, 1526 (1994).
- [2] S. Kashiwaya and Y. Tanaka, Tunnelling effects on surface bound states in unconventional superconductors, *Rep. Prog. Phys.* **63**, 1641 (2000).
- [3] M. Z. Hasan and C. L. Kane, Colloquium: Topological insulators, *Rev. Mod. Phys.* **82**, 3045 (2010).
- [4] X.-L. Qi and S.-C. Zhang, Topological insulators and superconductors, *Rev. Mod. Phys.* **83**, 1057 (2011).
- [5] Y. Tanaka, M. Sato, and N. Nagaosa, Symmetry and Topology in Superconductors -Odd-Frequency Pairing and Edge States-, *J. Phys. Soc. Jpn.* **83**, 011013 (2012).
- [6] M. Sato and Y. Ando, Topological superconductors: a review, *Rep. Prog. Phys.* **80**, 076501 (2017).
- [7] A. Haim and Y. Oreg, Time-reversal-invariant topological superconductivity in one and two dimensions, *Phys. Rep.* **825**, 1 (2019).
- [8] M. Sato, Y. Takahashi, and S. Fujimoto, Non-Abelian Topological Order in s -Wave Superfluids of Ultracold Fermionic Atoms, *Phys. Rev. Lett.* **103**, 020401 (2009).
- [9] A. Y. Kitaev, Unpaired Majorana fermions in quantum wires, *Phys. Usp.* **44**, 131 (2001).
- [10] R. M. Lutchyn, J. D. Sau, and S. DasSarma, Majorana Fermions and a Topological Phase Transition in Semiconductor-Superconductor Heterostructures, *Phys. Rev. Lett.* **105**, 077001 (2010).
- [11] Y. Oreg, G. Refael, and F. von Oppen, Helical Liquids and Majorana Bound States in Quantum Wires, *Phys. Rev. Lett.* **105**, 177002 (2010).
- [12] A. Cook and M. Franz, Majorana fermions in a topological-insulator nanowire proximity-coupled to an s -wave superconductor, *Phys. Rev. B* **84**, 201105(R) (2011).
- [13] J. Alicea, New directions in the pursuit of Majorana fermions in solid state systems, *Rep. Prog. Phys.* **75**, 076501 (2012).
- [14] V. Mourik, K. Zuo, S. M. Frolov, S. R. Plissard, E. P. A. M. Bakkers, and L. P. Kouwenhoven, Signatures of Majorana Fermions in Hybrid Superconductor-Semiconductor Nanowire Devices, *Science* **336**, 1003 (2014).
- [15] G. E. Volovik, Fermion zero modes on vortices in chiral superconductors, *JETP Lett.* **70**, 609 (1999).
- [16] N. Read and D. Green, Paired states of fermions in two dimensions with breaking of parity and time-reversal symmetries and the fractional quantum Hall effect, *Phys. Rev. B* **61**, 10267 (2000).
- [17] S. DasSarma, C. Nayak, and S. Tewari, Proposal to stabilize and detect half-quantum vortices in strontium ruthenate thin films: Non-abelian braiding statistics of vortices in a $p_x + ip_y$ superconductor, *Phys. Rev. B* **73**, 220502(R) (2006).
- [18] L. Fu and C. L. Kane, Superconducting proximity effect and majorana fermions at the surface of a topological insulator, *Phys. Rev. Lett.* **100**, 096407 (2008).
- [19] C. Nayak, S. H. Simon, A. Stern, M. Freedman, and S. DasSarma, Non-Abelian anyons and topological quantum computation, *Rev. Mod. Phys.* **80**, 1083 (2008).
- [20] D. Aasen, M. Hell, R. V. Mishmash, A. Higginbotham, J. Danon, M. Leijnse, T. S. Jespersen, J. A. Folk, C. M. Marcus, K. Flensberg, and J. Alicea, Milestones Toward Majorana-Based Quantum Computing, *Phys. Rev. X* **6**, 031016 (2016).
- [21] H. Sumiyoshi and S. Fujimoto, Quantum Thermal Hall Effect in a Time-Reversal-Symmetry-Broken Topological Superconductor in Two Dimensions: Approach from Bulk Calculations, *J. Phys. Soc. Jpn.* **82**, 023602 (2013).
- [22] K. Nomura, S. Ryu, A. Furusaki, and N. Nagaosa, Cross-Correlated Responses of Topological Superconductors and Superfluids, *Phys. Rev. Lett.* **108**, 026802 (2012).
- [23] Y. Shimizu, A. Yamakage, and K. Nomura, Quantum thermal Hall effect of Majorana fermions on the surface of superconducting topological insulators, *Phys. Rev. B* **91**, 195139 (2015).
- [24] J. J. He, Y. Tanaka, and N. Nagaosa, Optical responses of chiral majorana edge states in two-dimensional topological superconductors, *Phys. Rev. Lett.* **126**, 237002 (2021).
- [25] J. J. He and N. Nagaosa, Local Raman spectroscopy of chiral Majorana edge modes in Kitaev spin liquids and topological superconductors, *Phys. Rev. B* **103**, L241109 (2021).
- [26] T. Tsuneto, Ultrasonic attenuation in superconductors, *Phys. Rev.* **121**, 402 (1961).
- [27] L. P. Kadanoff and I. I. Falko, Ultrasonic attenuation in superconductors containing magnetic impurities, *Phys. Rev.* **136**, A1170 (1964).
- [28] B. Lüthi, Ultrasonics in superconductors, in *Physical Acoustics in the Solid State* (Springer, Berlin, 2005).
- [29] Y. Yamazaki, S. Kobayashi, and A. Yamakage, Magnetic Response of Majorana Kramers Pairs Protected by \mathbb{Z}_2 Invariants, *J. Phys. Soc. Jpn.* **89**, 043703 (2020).
- [30] S. Kobayashi, Y. Yamazaki, A. Yamakage, and M. Sato, Majorana multipole response: General theory and application to wallpaper groups, *Phys. Rev. B* **103**, 224504 (2021).
- [31] Y. Yamazaki, S. Kobayashi, and A. Yamakage, Electric Multipoles of Double Majorana Kramers Pairs, *J. Phys. Soc. Jpn.* **90**, 073701 (2021).

- [32] M. Oudah, A. Ikeda, J. N. Hausmann, S. Yonezawa, T. Fukumoto, S. Kobayashi, M. Sato, and Y. Maeno, Superconductivity in the antiperovskite Dirac-metal oxide $\text{Sr}_{3-x}\text{SnO}$, *Nat. Commun.* **7**, 13617 (2016).
- [33] T. Kawakami, T. Okamura, S. Kobayashi, and M. Sato, Topological Crystalline Materials of $J = 3/2$ Electrons: Antiperovskites, Dirac Points, and High Winding Topological Superconductivity, *Phys. Rev. X* **8**, 041026 (2018).
- [34] A. Widera and H. Schäfer, Übergangsformen zwischen zintlphasen und echten salzen: Die verbindungen A_3BO (MIT A = Ca, Sr, Ba und B = Sn, Pb), *Mater. Res. Bull.* **15**, 1805 (1980).
- [35] J. Nuss, C. Mühle, K. Hayama, V. Abdolazimi, and H. Takagi, Tilting structures in inverse perovskites, M_3TtO (M = Ca, Sr, Ba, Eu; Tt = Si, Ge, Sn, Pb), *Acta Cryst. B* **71**, 300 (2015).
- [36] T. Kariyado and M. Ogata, Three-Dimensional Dirac Electrons at the Fermi Energy in Cubic Inverse Perovskites: Ca_3PbO and Its Family, *J. Phys. Soc. Jpn.* **80**, 083704 (2011).
- [37] T. Kariyado and M. Ogata, Low-Energy Effective Hamiltonian and the Surface States of Ca_3PbO , *J. Phys. Soc. Jpn.* **81**, 064701 (2012).
- [38] T. H. Hsieh, J. Liu, and L. Fu, Topological crystalline insulators and Dirac octets in antiperovskites, *Phys. Rev. B* **90**, 081112(R) (2014).
- [39] See the Supplemental Material: I. Effective Hamiltonian on the (001) surface of antiperovskite, II. Spin current induced by dynamic strain.
- [40] T. Funato and M. Matsuo, Acoustic Rashba–Edelstein effect, *J. Magn. Magn. Mater.* **540**, 168436 (2021).
- [41] L. Elcoro, B. Bradlyn, Z. Wang, M. G. Vergniory, J. Cano, C. Felser, B. A. Bernevig, D. Orobengoa, G. de la Flor, and M. I. Aroyo, Double crystallographic groups and their representations on the Bilbao Crystallographic Server, *J Appl. Cryst.* **50**, 1457 (2017).
- [42] D. Kobayashi, T. Yoshikawa, M. Matsuo, R. Iguchi, S. Maekawa, E. Saitoh, and Y. Nozaki, Spin Current Generation Using a Surface Acoustic Wave Generated via Spin-Rotation Coupling, *Phys. Rev. Lett.* **119**, 077202 (2017).
- [43] S. Tateno, G. Okano, M. Matsuo, and Y. Nozaki, Electrical evaluation of the alternating spin current generated via spin-vorticity coupling, *Phys. Rev. B* **102**, 104406 (2020).
- [44] T. Kawada, T. Funato, H. Kohno, and M. Hayashi, Acoustic spin Hall effect in strong spin-orbit metals, *Sci. Adv.* **7**, eabd9697 (2021).